

Encapsulation technique efficiency in high zinc chloride concentration clayey soil with traditional agents

Eficiência da técnica de encapsulamento em solo argiloso com elevadas concentrações de cloreto de zinco com agentes tradicionais

Isabel Amado Perez¹, José Wilson dos Santos Ferreira^{2*} , José Adriano Cardoso Malko¹ ,
Maria Isabel Pais Silva¹ , Michéle Dal Toé Casagrande² 

ABSTRACT

Although the encapsulation technique has been used in environmental remediation for over three decades, there are few studies evaluating its efficacy for high contaminant concentrations. Therefore, this study aims to evaluate the encapsulation technique efficiency of clayey soil contaminated with 5% and 10% of zinc chloride, using lime and cement. Chemical, mechanical, mineralogical, and microscopic analyses were performed for pure, contaminated, and encapsulated soil, based on X-ray fluorescence (XRF/EDX), unconfined compression strength (UCS), atomic absorption spectrometry (AAS), scanning electron microscopy/energy dispersive X-ray spectrometer (SEM/EDS), and X-ray micro-computed tomography (micro-CT) tests. Although chemical interactions between zinc and lime negatively affected the gains when compared to cement, both encapsulating agents increased the strength over the curing periods of 7, 28, and 60 days. The leachates presented a significant reduction in the contaminant concentration, above 77% for critical experimental conditions. The contaminant reduced the presence of chemical elements that compose the soil matrix, consequently causing the voids to increase; in contrast, pozzolanic reactions promoted by the addition of lime and cement resulted in homogeneous voids distribution, enhancing the mechanical behavior and the capability of zinc chloride retention.

Keywords: encapsulation; contaminated soil; leaching; remediation; microstructural analysis.

RESUMO

Ainda que a técnica de encapsulamento seja usada na remediação ambiental há mais de três décadas, existem poucos estudos que avaliam sua eficácia para altas concentrações de contaminantes. Assim, este trabalho tem como objetivo avaliar a eficiência da técnica de encapsulamento de solo argiloso contaminado com 5 e 10% de cloreto de zinco, utilizando cal e cimento. Análises química, mecânica, mineralógica e microscópica foram realizadas para o solo puro, contaminado e encapsulado, com base em ensaios de fluorescência de raios X, resistência à compressão simples, espectrometria de absorção atômica, microscopia eletrônica de varredura e microtomografia de raios X. Ambos os agentes encapsulantes aumentaram a resistência ao longo dos períodos de cura de sete, 28 e 60 dias, embora as interações químicas entre zinco e cal tenham afetado negativamente os ganhos quando comparados ao do cimento. Os lixiviados apresentaram redução significativa na concentração de zinco, acima de 77% para condições experimentais críticas. O contaminante reduziu a presença de elementos químicos que compõem a matriz do solo, fazendo com que os vazios aumentassem; por outro lado, as reações pozolânicas promovidas pela adição de cal e cimento resultaram em distribuição de vazios mais homogênea, melhorando o comportamento mecânico e a capacidade de retenção de cloreto de zinco.

Palavras-chave: encapsulamento; solo contaminado; lixiviação; remediação; análise microestrutural.

INTRODUCTION

Metal pollution in soil, which has become a worldwide environmental concern, is mainly associated with factors such as fast-paced industrialization,

growing urbanization, modernized agricultural and mining practices, and inadequate methods of tailing disposal (KLIMEK, 2012; DU *et al.*, 2014a; 2014b).

¹Pontifícia Universidade Católica do Rio de Janeiro - Rio de Janeiro (RJ), Brazil.

²Universidade de Brasília - Brasília (DF), Brazil.

*Corresponding author: ferreira.jose@aluno.unb.br

Conflicts of interest: the authors declare no conflicts of interest.

Funding: Conselho Nacional de Desenvolvimento Científico e Tecnológico (CNPq), Process 141127/2019-8 and 426100/2018-2.

Received: 07/06/2020 - **Accepted:** 10/01/2021 - **Reg. ABES:** 20200241

Depending on its concentration, zinc – a metal that is widely used in industrial activities – can be seen as both a health-essential micronutrient and a potentially toxic micropollutant. One of the health risks caused by this element is the formation of a protein that, in excess, causes plaques to accumulate in the brain in a neurotoxicity process responsible for Alzheimer's disease (HORNING *et al.*, 2000; DUCE *et al.*, 2010).

In the past few decades, the environmental policies developed in Brazil regarding soil usage for final waste disposal, especially for hazardous waste, have become increasingly strict, requiring the use of safer and more efficient methods for management and disposal. According to the Environmental Protection Agency (EPA, 2017) the most commonly used in situ remediation techniques are soil vapor extraction, chemical and thermal treatments, and bioremediation and solidification/stabilization (KEMPA *et al.*, 2013; NEWSOME *et al.*, 2014; PEDERSEN *et al.*, 2018; LIU *et al.*, 2018; LI *et al.*, 2019).

Evaluating the effect of the vapor technique on the geological engineering properties of a tar contaminated area, Kempa *et al.* (2013) justified the impossibility of soil extraction as a preponderant factor for choosing the techniques, being added with Pedersen *et al.*'s (2018) other factors, such as soil properties, pollutant composition and amount, soil pollutant binding, and cost-effectiveness. In this regard, an economical treatment is the soil encapsulation technique, also called solidification/stabilization (S/S), still underexplored in Brazil, even though it has been used for over 30 years in countries like United States, Japan, and England.

The solidification process involves binding the residues into a solid block of materials (soil + contaminant + encapsulating agent) that becomes less water permeable than the residue in its pure form, whereas the stabilization process is characterized by a chemical reaction that decreases the contaminant's mobility, solubility, and toxicity, reducing the probability of the pollutant leaching into the environment and preventing or delaying the release of the hazardous chemical by-products from contaminated soils (CHEN *et al.*, 2009; HALE *et al.*, 2012; EPA, 2017).

Several studies have addressed the soil encapsulation technique, analyzing the soil's mechanical and hydraulic behavior and the leachate's characteristics (DU *et al.*, 2014b; GLASSER, 1997; OLMO *et al.*, 2001; YIN *et al.*, 2006; WEI *et al.*, 2011; WEI *et al.*, 2012; DU *et al.*, 2013; NIU *et al.*, 2018; MCKINLEY *et al.*, 2001), but there are few studies about the effect of high concentrations of contaminant on the mixture's mechanical and microstructural behavior.

As such, motivated by two accidents that happened recently in mineral processing industries in Brazil, this research evaluated the efficiency of the encapsulating technique applied to clayey soil contaminated with high concentrations of zinc chloride, using lime and cement as encapsulating agents and employing different curing periods. Besides the physical, mechanical, and hydraulic analyses, chemical and microscopic tests were conducted in order to seek a better understanding of the interaction between the components in the behavior of the mixtures.

METHODOLOGY

Experimental program

Materials

The soil used in this study was a yellowish-red tropical colluvial clay, extracted from the Experimental Field II of the Pontifical Catholic University of Rio de

Janeiro, Brazil. Its mineral composition consisted mainly of kaolinite clay mineral ($\text{Al}_2\text{Si}_2\text{O}_5(\text{OH})_4$), quartz (SiO_2), iron (Fe_2O_3), titanium (TiO_2), and aluminum oxides (Al_2O_3).

Physical characterization tests were carried out for determining the index properties of clayey soil and particle size distribution by sedimentation analysis (Figure 1). The Atterberg limits for the portion passing through no. 40 sieve have are 52% for liquid and 34% for plastics. The specific gravity of solids is 2.69, in agreement with the values obtained by other authors using the same soil (Ramirez *et al.*, 2015; Louzada *et al.*, 2019). According to the Unified Soil Classification System (USCS), the soil is classified as silt of high plasticity (MH).

For the contaminant, zinc chloride was selected due to its wide utilization in oil refining, food additives, electrotyping, as well as in the catalyst, metallurgical, and dye industries, and as a dehydrating and condensing agent in organic synthesis. The product was acquired from a specialized company, presenting a zinc chloride minimum concentration of 96%.

To act as encapsulating agents in the remediation process, Portland cement of high initial strength (Type III) and calcitic hydrated lime (CH-III) were selected. Distilled water was used for characterization tests, while tap water was used for compaction tests and molding the mixtures.

Testing methods

From an actual case of zinc contamination occurred in the Bay of Sepetiba/Rio de Janeiro by the Mercantile and Industrial Company Ingá, and percentages of zinc concentration identified in the contaminated soil by Delmonte (2010), amounts of 5% and 10% of solid zinc chloride, in relation to the mixture total dry weight, were added to investigate high zinc concentration-contaminated land. The cement and lime contents were established based on preliminary tests and literature recommendations (KNOP *et al.*, 2008). Table 1 summarizes the experimental conditions investigated and the symbols used. The molding parameters, maximum dry density (ρ_d max) and optimum moisture content (ω_{opt}), were obtained from compaction tests, using normal energy in the Proctor cylinder (ASTM D698, 2012). Based on this, unconfined compressive strength (UCS) tests were carried out in duplicate for each experimental condition, using specimens with a diameter of 50 mm and height of 100 mm, and curing periods of 0, 7, 28, and 60 days (ASTM D2166/D2166M, 2016; ASTM D1633, 2017). Before the destructive stage, the specimens were immersed in water for 4 h in order to approach the saturation condition. This procedure was not performed in samples without curing time because of the occurrence of disaggregation.

For the characterization of the chemical elements present in the natural, contaminated, and encapsulated soil, the materials were mixed following the proportions

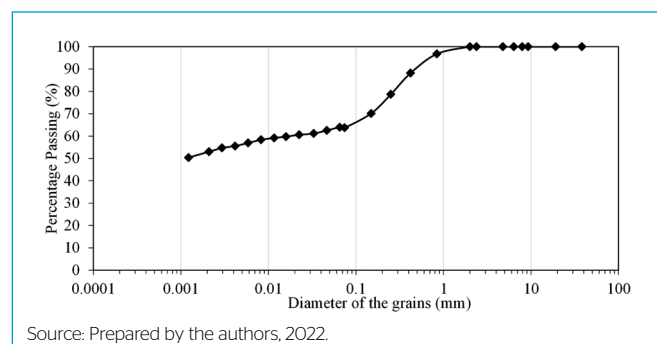


Figure 1 - Particle size distribution curve of the pure soil.

shown in Table 1, and 2 g was used for testing in the X-ray fluorescence spectrometry (XRF/EDX on a Shimadzu EDX-700 spectrometer. The same equipment was used for the leachate tests, from specimens molded with a diameter of 40.4 mm in and height of 78.0 mm in and 3 curing period of 3 days. Using an adapted permeameter, the water percolation occurred in a saturated up-flow mode by maintaining a difference of 50 kPa between the top and base pressure (ASTM D4874, 2014). The confining stress was 5 kPa higher than the pressure at the base, around 350–400 kPa. In addition to identifying the chemical elements in the collected leachates, zinc concentration was quantified by atomic absorption spectrometry (AAS) on an Analytikjena ContrAA 300 model in order to verify the technique's efficiency and compliance with the standards of zinc concentration established by the National Environment Council resolutions (BRAZIL, 2008; 2009).

The concern about the zinc effects on the structural arrangement of soil particles and interactions with the encapsulating agent motivated microstructural tests by scanning electron microscopy (SEM) connected to energy dispersive X-ray spectrometer (EDS) and X-ray micro-computed tomography (micro-CT)

for S_{100} , $S_{95}Zn_5$, $S_{90}Zn_{10}$, $S_{85}Zn_{10}C_{10}$, and $S_{85}Zn_5L_{10}$, based on the mixtures that displayed the highest efficiency in the chemical analyses. Micro-CT is a non-destructive and noninvasive technique, allowing to carry out studies in three dimensions (3D) in a micrometric scale to investigate phenomena in soil physics, based on computer-processed combinations of X-ray images taken from different angles to produce cross-sectional images of specific areas.

For this purpose, samples were made in a metallic mold with a diameter of 10 mm and height of 28.6 mm, in and were then wrapped in plastic wrap, tagged, and placed in a hermetically sealed container to avoid variations in moisture during the curing periods of 14 (SEM and EDS) and 18 days (micro-CT).

Test results and analysis

The compaction curves and parameters are shown in Figure 2 and Table 2. The presence and increase of soil contaminant concentration (S_{100} , $S_{95}Zn_5$, and $S_{90}Zn_{10}$) raised the maximum dry density and decreased the optimum moisture content, which is explained by the higher zinc specific gravity (2.91) when compared to the soil solids (2.69), as well as the presence of water molecules in its composition, reducing the water amount required.

Once the encapsulating agents were used in contaminated soil, the mixtures demanded more water, due to the increase of the surface to be hydrated. Considering the same amount of lime and cement, with $ZnCl_2$ growth from 5% to 10%, a decrease in this parameter can be noted, confirming the previous observation. Also, the increase in cement or lime content resulted in a maximum decrease in dry density.

The establishment of additional trends was affected by the chemical interactions between soil, zinc, and encapsulating agents, expressed by the variability

Table 1 - Ratio of soil, contaminant, and encapsulating agent.

Materials / Mixtures	Proportion of Materials			
	Soil (%)	Zinc chloride (%)	Lime (%)	Cement (%)
S_{100}	100	0	0	0
$S_{95}Zn_5$	95	5	-	-
$S_{90}Zn_{10}$	90	10	-	-
$S_{90}Zn_5L_5$	90	5	5	-
$S_{85}Zn_5L_{10}$	85	5	10	-
$S_{85}Zn_{10}L_5$	85	10	5	-
$S_{80}Zn_{10}L_{10}$	80	10	10	-
$S_{90}Zn_5C_5$	90	5	-	5
$S_{85}Zn_5C_{10}$	85	5	-	10
$S_{85}Zn_{10}C_5$	85	10	-	5
$S_{80}Zn_{10}C_{10}$	80	10	-	10

Source: Prepared by the authors, 2022.

Table 2 - Soil and mixture compaction parameters.

Materials/ Mixtures	Compaction Parameters	
	Optimum moisture content (%)	Maximum dry density ($g\ cm^{-3}$)
S_{100}	26.3	1.555
$S_{95}Zn_5$	21.5	1.608
$C_{90}Zn_{10}$	19.4	1.729
$S_{90}Zn_5L_5$	23.2	1.534
$S_{85}Zn_5L_{10}$	24.2	1.512
$S_{85}Zn_{10}L_5$	21.5	1.616
$S_{80}Zn_{10}L_{10}$	21.1	1.514
$S_{90}Zn_5C_5$	22.7	1.626
$S_{85}Zn_5C_{10}$	23	1.523
$S_{85}Zn_{10}C_5$	20.6	1.615
$S_{80}Zn_{10}C_{10}$	21.7	1.572

Source: Prepared by the authors, 2022.

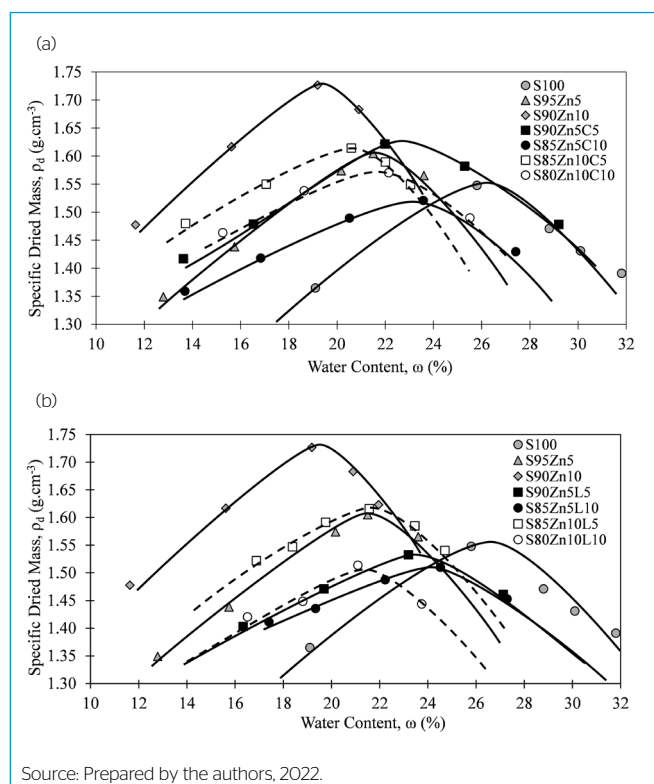
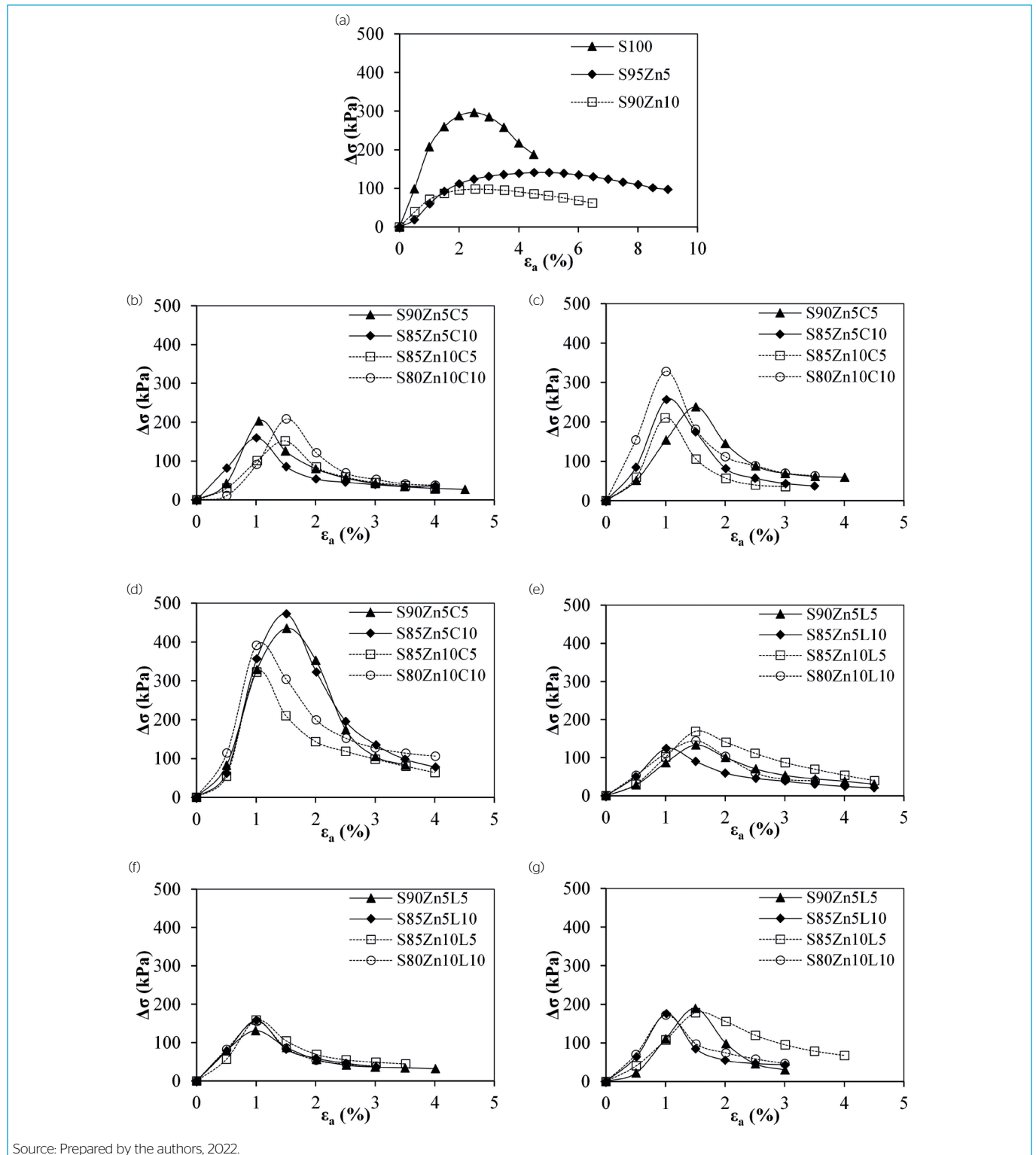


Figure 2 - Compaction curves of the pure, contaminated, and encapsulated soil with (a) cement and (b) lime

on both parameters. Hence, the determination of mixtures parameters is a requested step, in contrary to the tendency shown in the studies of Jiang *et al.* (2014) and Du *et al.* (2014b), which employed the results obtained in the raw soil for the encapsulated mixtures.

Figure 3a shows the stress-strain curves of the non-contaminated and contaminated soil with 5% and 10% of zinc chloride. The presence of the contaminant altered material's behavior from brittle characteristic to behave like a ductile material a significantly drops in peak stress. The soil's unconfined compressive



Source: Prepared by the authors, 2022.

Figure 3 - Stress-strain curves of the mixtures encapsulated by cement and lime with curing periods of 0, 7, 28, and 60 days: (a) pure and contaminated soil/0 days; (b) mix with cement/7 days; (c) mix with cement/28 days; (d) mix with cement/60 days; (e) mix with lime/7 days; (f) mix with lime/28 days; and (g) mix with lime/60 days.

strength of 296.7 kPa was reduced to 141.1 kPa ($S_{95}Zn_5$) and 98.2 kPa ($S_{90}Zn_{10}$) in the presence of zinc.

The stress-strain curves of contaminated soil encapsulated by cement and lime with curing periods of 7, 28, and 60 days are shown in Figure 3b–3g. In general, the growth of peak stress is observed with the increase in the curing period. The strength improvement for both agents is based on hydration process, ion exchange, flocculation, and interaction between the minerals of the soil and encapsulating agents, which produces a cementing compound named pozzolans (BELL, 1996; SCRIVENER *et al.*, 2019).

In view of contaminated soil encapsulated by lime, the strength increments with curing time were inferior to the cement mixtures. It can be associated with reactions among zinc chloride and lime in the early day, affecting the pozzolanic reactions, which requires considerably more time than cement to produce a cementing compound.

From the stress-strain curves, unconfined compressive strengths are presented in Figure 4. As previously mentioned, the mixtures that received the addition of cement had a significant increase in unconfined compressive strength. During 7 and 28 days, the mixture with the maximum amount of zinc and cement presented a higher strength ($S_{80}Zn_{10}C_{10}$). Even though zinc reacts with cement components, as pointed out by Yousuf *et al.* (1995) and Du *et al.* (2013), the behavior was governed by the hydration of the tricalcium silicate of the cement, primarily responsible for resistance at early ages.

At 60 days of curing, the $S_{85}Zn_5C_{10}$ exhibited superior resistance which as expected, since this mixture contains the maximum of cement and the minimum of zinc chloride. Consequently, the mixture $S_{85}Zn_{10}C_5$ originated as the least resistant mixture for all the curing periods evaluated.

Nevertheless, the addition of cement improved the strength of both zinc concentrations in the soil, suggesting that cement is effective not only for low concentrations of zinc as reported by Du *et al.* (2014b) but also for high concentrations.

In the mixtures that had lime as the encapsulating agent, it can be observed that despite the increase in strength with longer curing periods, this variation was not as significant as it was in the behavior of the mixtures with cement, which hinders the establishment of a general trend. The variability can be attributed to reactions between zinc chloride and lime in the mixtures, which limited and/or delayed the lime's reactions and reduced the number of cementitious products (Du *et al.*, 2013).

Even so, it is possible to notice that the behavior of the mixtures with 10% of lime was better characterized and pointed to an increase in strength with longer curing periods. For the longest curing period (60 days), it is seen that the UCS maintains stability, independently of the zinc or lime content. The same trend was noted by Li *et al.* (2019) from 2% of zinc.

The results from the chemical analyses of the mixtures (Table 3), obtained through X-ray fluorescence, show that the increase in the amount of lime and cement resulted in a lower ratio of zinc in the mixtures. In contrast, reductions were observed in the amounts of iron, aluminum, and silicon, elements that compose the soil structure, indicating an alteration in the soil matrix.

The chemical results collected in the leachates are presented in Table 4. It should be pointed out that the results shown in both tables are presented in percentages pertaining to the ratios of elements present in the mixture.

In the leachates of the encapsulated soil with lime, the percentage of chlorine was higher than in the contaminated soil due to reactions between zinc

Table 3 - Chemical analyses of the materials and mixtures.

Materials / Mixtures	Elements of mixtures (%)							
	Fe	Al	Si	Ti	Zn	Ca	Cl	Mg
S_{100}	43.2	25.8	25.2	3.7	ND	ND	ND	ND
$ClZn_2$	ND	ND	ND	ND	74.4	0.2	25.1	ND
Cement	5.3	1.5	3.3	0.3	ND	87.4	ND	ND
Lime	0.5	ND	ND	ND	ND	86.7	ND	11.5
$S_{95}Zn_5$	38.5	27.2	22.3	3.7	6.6	ND	ND	ND
$S_{90}Zn_{10}$	40.0	28.2	24.3	3.9	1.6	ND	ND	ND
$S_{90}Zn_5C_5$	38.4	19.7	16.3	3.7	0.9	18.8	ND	ND
$S_{85}Zn_{15}C_{10}$	31.3	14.6	12.6	3.3	0.4	35.9	ND	ND
$S_{85}Zn_{10}C_5$	37.1	21.1	18.6	3.7	1.2	16.4	ND	ND
$S_{80}Zn_{10}C_{10}$	28.6	12.5	10.9	3.0	0.5	42.4	ND	ND
$S_{90}Zn_5L_5$	34.0	22.0	18.2	3.5	8.2	8.9	3.5	ND
$S_{85}Zn_5L_{10}$	33.1	17.4	14.7	3.6	5.9	21.2	ND	3.4
$S_{85}Zn_{10}L_5$	30.6	20.5	16.9	3.0	13.8	10.1	4.2	ND
$S_{80}Zn_{10}L_{10}$	31.6	12.2	9.5	3.2	0.6	35.6	ND	6.1

ND, Not detected. Source: Prepared by the authors, 2022.

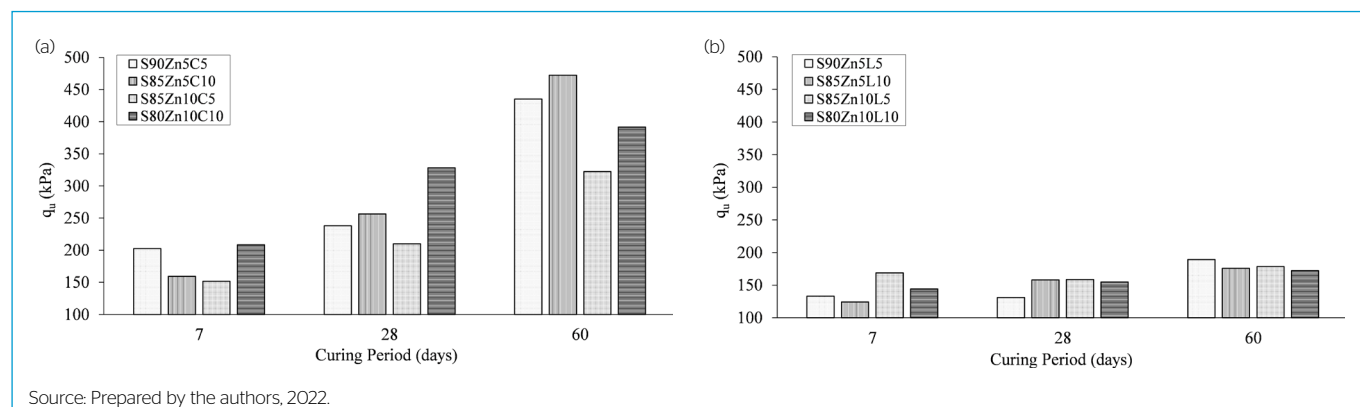


Figure 4 - Variation of unconfined compressive strengths (q_u) according to the curing time for the encapsulated soil with (a) cement and (b) lime.

chloride and lime, resulting in calcium chloride and zinc oxide ($ZnCl_2 + CaO \rightarrow ZnO + CaCl_2$).

The results from the AAS conducted to quantify the concentration of zinc in the leachates of the mixtures (in $mg L^{-1}$) are shown in Figure 5. Also, the zinc concentration restrictions of 5000 and 10500 $mg L^{-1}$, established by National Environment Council resolutions are also presented.

The concentration of most encapsulated contaminated soil was below the limits specified in both resolutions, with the exception of mixtures $S_{85}Zn_{10}C_5$ and $S_{85}Zn_{10}L_5$, indicating that a ratio of lime and cement lower than 5% is inefficient in a remediation process with a zinc concentration of 10%.

It should be noted that both X-ray fluorescence and AAS methodology for the leachate analysis resulted in the same efficiency pattern of the mixtures, from the most effective to the least effective: $S_{85}Zn_5L_{10}$, $S_{80}Zn_{10}C_{10}$, $S_{85}Zn_5C_{10}$, $S_{90}Zn_5L_5$, $S_{80}Zn_{10}L_{10}$, $S_{90}Zn_5C_5$, $S_{85}Zn_{10}C_5$, and $S_{85}Zn_{10}L_5$.

In comparison to the concentrations presented by the leachate of the contaminated soil, 21.110 $mg L^{-1}$ for $S_{95}Zn_5$ and 53.060 $mg L^{-1}$ for $S_{90}Zn_{10}$,

Table 4 - Ratio of the elements present in the leachates.

Materials / Mixtures	Elements of mixtures (%)						
	Zn	Cl	Ca	S	Fe	Al	Si
S_{100}	ND	ND	ND	0.7	43.2	25.8	25.2
$S_{95}Zn_5$	73.9	22.9	0.9	1.4	ND	ND	0.8
$S_{90}Zn_{10}$	72.2	26.8	0.8	0.2	ND	ND	ND
$S_{90}Zn_5C_5$	15.6	28.5	55.6	0.2	ND	ND	ND
$S_{85}Zn_5C_{10}$	1.3	27.8	70.1	0.2	ND	ND	ND
$S_{85}Zn_{10}C_5$	35.0	29.3	34.2	0.8	ND	0.4	ND
$S_{80}Zn_{10}C_{10}$	0.6	28.4	69.5	0.6	ND	0.4	ND
$S_{90}Zn_5L_5$	1.3	42.7	49.2	0.2	ND	ND	ND
$S_{85}Zn_5L_{10}$	ND	31.4	67.0	1.0	ND	ND	0.6
$S_{85}Zn_{10}L_5$	37.0	36.9	24.8	0.7	ND	ND	0.5
$S_{80}Zn_{10}L_{10}$	2.0	46.3	49.8	1.1	ND	0.8	ND

ND, Not detected. Source: Prepared by the authors, 2022.

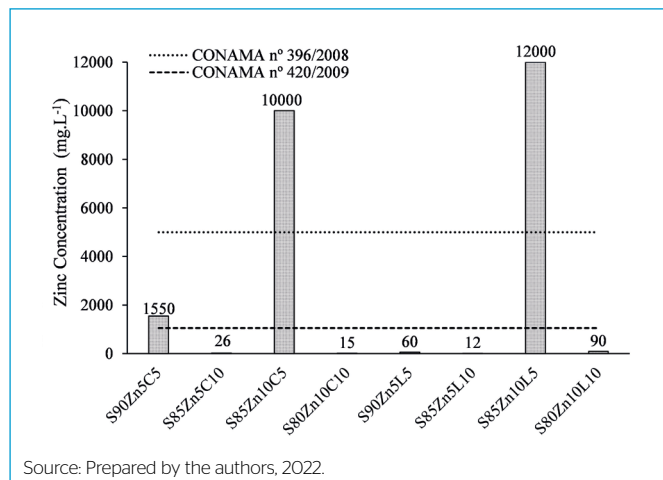


Figure 5 - Concentration of zinc in the leachate and limits established in CONAMA's resolutions.

the capability to retain zinc chloride (Figure 6) was satisfactory, showing above 77% in critical experimental conditions, i.e., the superior amounts of contaminant and inferior encapsulant. The efficiency was above 99% for mixtures that complied with both of CONAMA's directives, thus proving the efficacy of the encapsulating technique with traditional agents in high zinc concentrations.

Figure 7 presents the microstructure of the soil with 5% and 10% of $ZnCl_2$, as well as the mixtures that presented a higher capacity to retain the contaminant ($S_{85}Zn_5L_{10}$ and $S_{80}Zn_{10}C_{10}$).

It is seen as a denser matrix for the pure soil (Figure 7a), where the clods were well bound with few voids between them. For the contaminated soil, the voids were more evident with the presence of the contaminant ($S_{95}Zn_5$ in Figure 7b and $S_{90}Zn_{10}$ in Figure 7c), which explains the drop in resistance.

Small agglomerations were formed by lime incorporation (Figure 7d), especially in the mixture containing cement (Figure 7e), due to the hydration of the calcium silicates and the pozzolanic reactions, which resulted in flocculation and cementation on the surface and around the clay particles. The resulting structure not only makes the soil stiffer, as demonstrated in the unconfined compression strength results, but also encapsulates the contaminant. Figure 7f shows the matrix of mixture $S_{80}Zn_{10}C_{10}$ with an approximation of 100', where the formation of a laminated structure can be seen.

Points 1, 2, and 3 in Figure 7 were selected to evaluate the distribution of the chemical elements using EDS (Figure 8). The soil exhibited peaks of silicon (Si), iron (Fe), aluminum (Al), and oxygen (O), which form their chemical base. In addition to the elements previously identified, the contaminated clay presented chlorine (Cl) and zinc (Zn), all of them in smaller proportions. For the soil encapsulated with cement, the spectrum displayed a peak of calcium (Ca), indicating the formation of cemented products.

In the micro-CT analyses, around 1000 two-dimensional (2D) images for each of the investigated conditions were collected and reduced to 200–300 for 3D conversion, disregarding the images captured at the top and bottom of the samples. Figure 9 demonstrates the solid particles and voids present in the raw (S_{100}), contaminated ($S_{95}Zn_5$), and encapsulated soil ($S_{85}Zn_5L_{10}$, $S_{80}Zn_{10}C_{10}$).

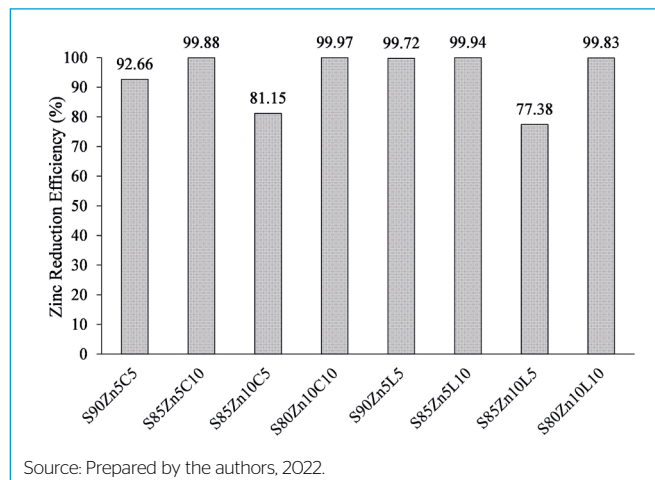
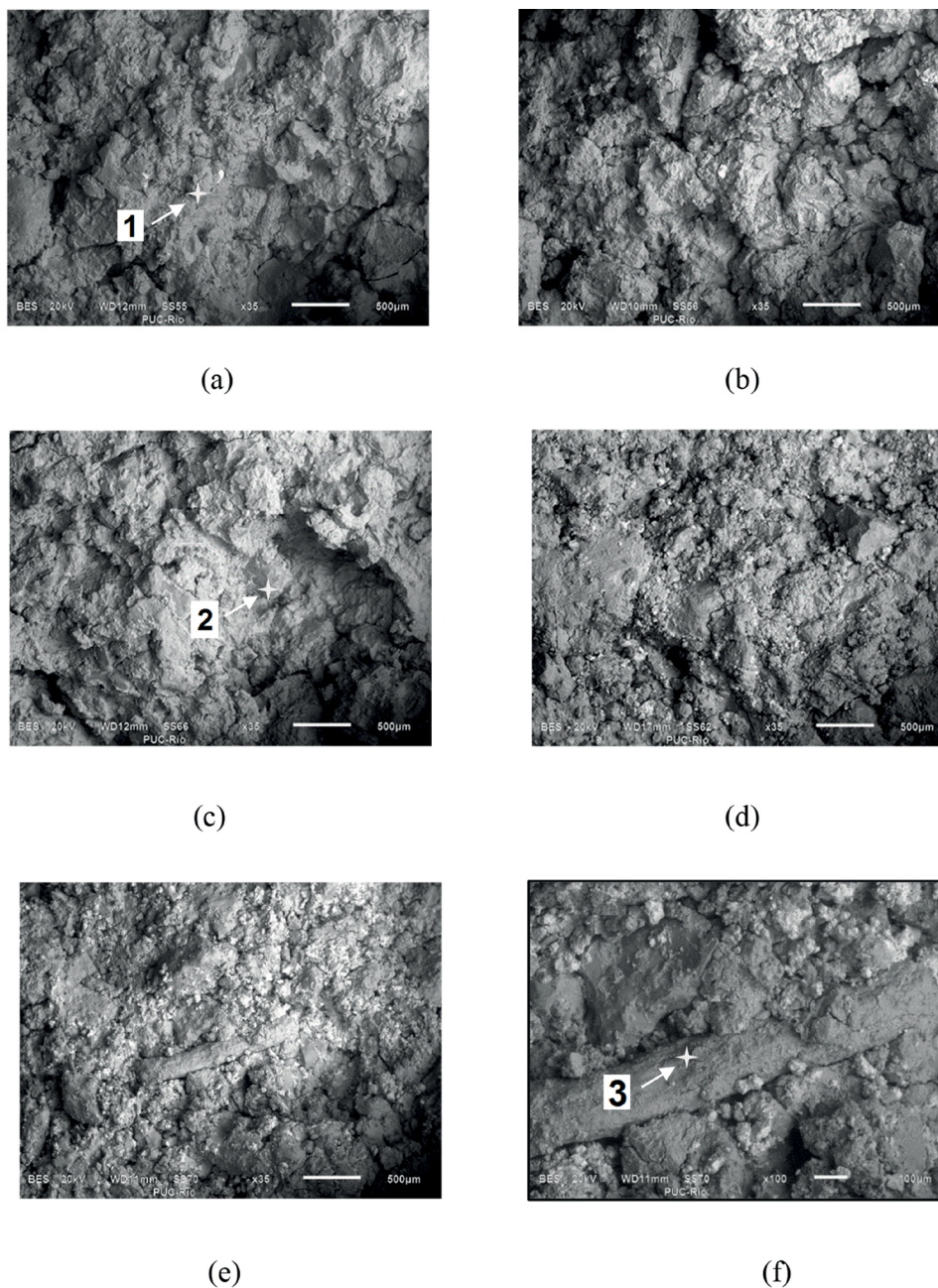


Figure 6 - Efficiency of zinc retention.



Source: Prepared by the authors, 2022.

Figure 7 – Scanning electron microscopy in samples of (a) $S_{100}, 35$; (b) $S_{95}Zn_5, 35$; (c) $S_{90}Zn_{10}, 35$; (d) $S_{85}Zn_{15}, 35$; (e) $S_{80}Zn_{10}C_{10}, 35$; and (f) $S_{80}Zn_{10}C_{10}, 100$.

The white particles presented in all conditions represent elements with a higher atomic density such as iron and zinc, which absorb more X-rays. From Figure 9a and 9b, it is noted that the zinc chloride presence resulted in a void increase, demonstrated by the black area.

As the encapsulating agent is added (Figure 9c and 9d), the bond between particles is improved by the presence of calcium and its cementing effect, which is evidenced by the appearance of gray particles. Such assumption comes from

the fact that this element has an intermediate atomic density and it had not been previously detected.

To analyze the distribution of the pores in each mixture, the black parts, representing the voids, were converted to white (Figure 10). Despite the fact that the contaminated soil encapsulated with cement and lime had a higher number of voids, the mixtures exhibited a more homogeneous distribution by virtue of the similar size of the voids, which was reflected in the improvement

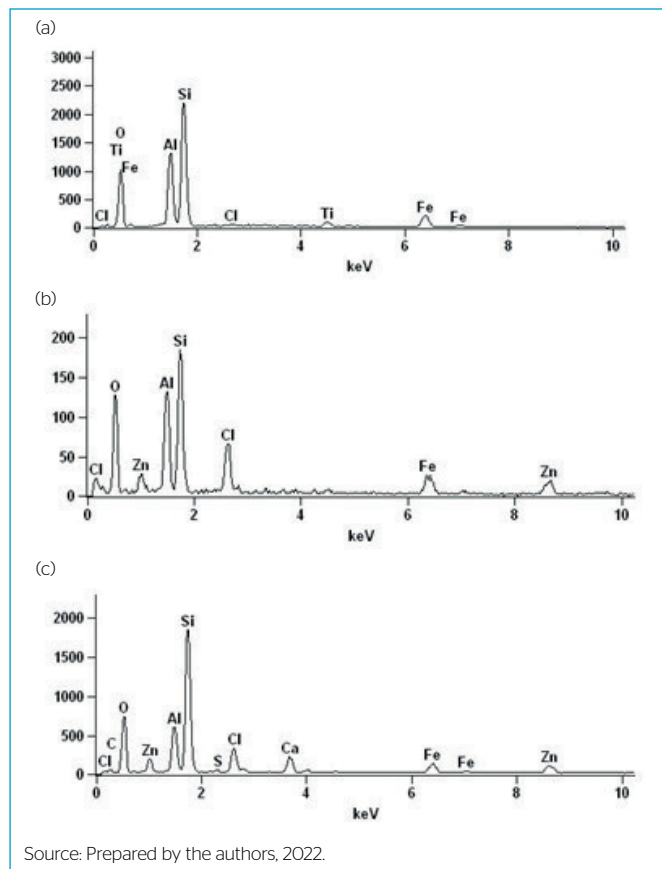


Figure 8 - Distribution of the chemical elements obtained with EDS: (a) Pure soil - Point (1) in Figure 7a; (b) $S_{90}Zn_{10}$ - Point (2) in Figure 7c; and (c) $S_{80}Zn_{10}C_{10}$ - Point (3) in Figure 7f.

of soil resistance. In contrast, the voids of the soil and contaminated soils were dispersed and presented larger sizes, characterizing a more heterogeneous and porous structure, affecting its support and retention capacity.

CONCLUDING REMARKS

Based on the results and analyses presented in the paper, it is possible to conclude that:

- The presence of $ZnCl_2$ in the soil significantly reduced its unconfined compressive strength. This behavior is believed to be caused by the increase in voids and the reduced presence of the chemical elements that compose the soil matrix, resulting in a more heterogeneous structure.
- The addition of lime and cement to the contaminated soil enhanced the mechanical behavior. For lime, this effect was not as significant in the mixtures, since reactions between the contaminant and the encapsulant agent gave rise to calcium chloride formation that increased the ratio of chlorine.
- The curing period was shown to be an important variable to increase the mechanical strength of contaminated soil encapsulated by cement, while the lime encapsulation did not show any significant differences with the increase of the curing period.
- Both encapsulation agents proved to be efficient in the mitigation of the leaching of high concentrations of zinc. Even though the void ratio was higher in the mixtures with lime and cement when compared to the

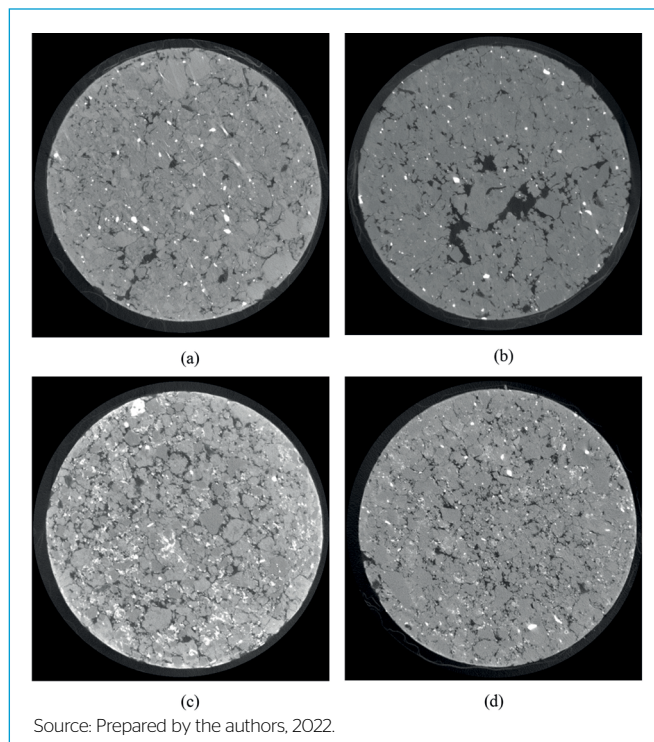


Figure 9 - Micro-CT conducted for (a) S_{100} ; (b) $S_{95}Zn_5$; (c) $S_{85}Zn_{15}L_{10}$; and (d) $S_{80}Zn_{10}C_{10}$.

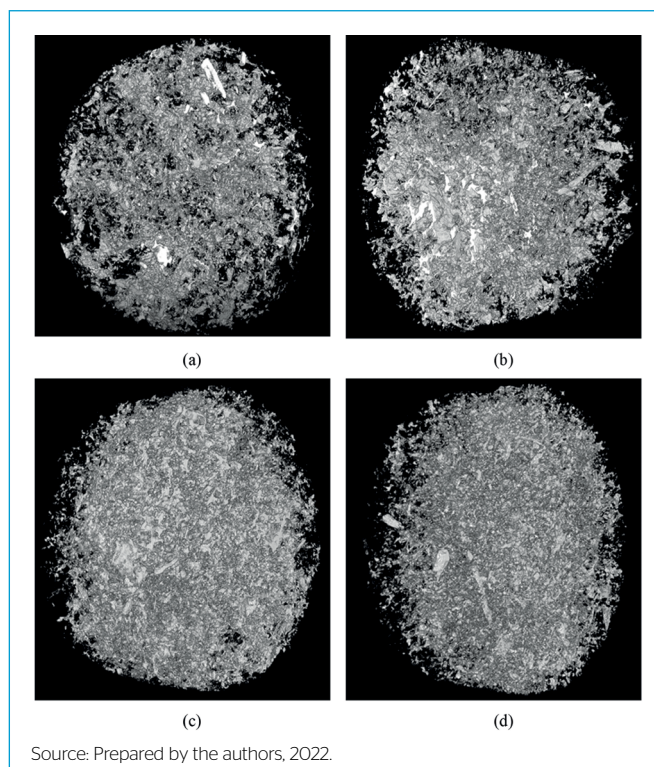


Figure 10 - Micro-CT representing the voids of (a) S_{100} ; (b) $S_{95}Zn_5$; (c) $S_{85}Zn_{15}L_{10}$; and (d) $S_{80}Zn_{10}C_{10}$.

pure soil, the encapsulating agents yielded a more homogeneous void distribution, improving the soil's mechanical behavior and its ability to retain the contaminant.

AUTHOR'S CONTRIBUTIONS

Perez, I.A.: Conceptualization, Investigation, Formal analysis; Ferreira J.W.S.: Conceptualization, Methodology, Investigation, Formal analysis, Writing – Original

draft preparation, review & editing; Malko J.A.C.: Writing – Original draft preparation; Silva M.I.P.: Investigation, Resources; Casagrande M.D.T.: Conceptualization, Resources, Supervision.

REFERÊNCIAS

- ASTM INTERNATIONAL. *Standard test methods for laboratory compaction characteristics of soil using standard effort (12 400 ft-lbf/ft³ (600 kN-m.m³)).* ASTM D698 - 12e2, West Conshohocken, PA, 2012. Available at: <<https://standards.globalspec.com/std/3846856/ASTM%20D698-12>>. Accessed on: 31 mar. 2022.
- ASTM International. *Standard test methods for leaching solid material in a column apparatus.* ASTM D4874 - 14, West Conshohocken, PA, 2014. Available at: <<https://standards.globalspec.com/std/3854564/astm-d4874-95-2014>>. Accessed on: 31 mar. 2022.
- ASTM International. *Standard test method for unconfined compressive strength of cohesive soil.* ASTM D2166/D2166M - 16, West Conshohocken, PA, 2016. Available at: <<https://standards.globalspec.com/std/3861763/astm-d2166-d2166m-16>>. Accessed on: 31 mar. 2022.
- ASTM International. *Standard test methods for compressive strength of molded soil-cement cylinders.* ASTM D1633 - 17, West Conshohocken, PA, 2017. Available at: <https://webstore.ansi.org/standards/astm/astmd163317?gclid=CjwKCAjwopWSBhB6EiwAjxmQDeXk3q8nWQyLZGNF16i03IZYYWn_Uo2Ylfaf_2_BG_1GYUd6xnSxHoCoPYQAvD_BwE>. Accessed on: 31 mar. 2022.
- BELL, F.G. Lime stabilization of clay minerals and soils. *Eng. Geol.*, v. 42, n. 4, p. 223 - 237, 1996. [https://doi.org/10.1016/0013-7952\(96\)00028-2](https://doi.org/10.1016/0013-7952(96)00028-2)
- BRASIL. Resolução nº. 396, de 3 de abril de 2008. Dispõe sobre a classificação e diretrizes ambientais para o enquadramento das águas subterrâneas e dá outras providências. Conselho Nacional do Meio Ambiente (CONAMA) - Ministério do Meio Ambiente. *Diário Oficial da União*, Brasília, DF, 2008.
- BRASIL. Resolução nº. 420, de 28 de dezembro de 2009. Dispõe sobre critérios e valores orientados de qualidade do solo quanto à presença de substâncias químicas e estabelece diretrizes para o gerenciamento ambiental de áreas contaminadas por essas substâncias em decorrência de atividades antrópicas. Conselho Nacional do Meio Ambiente (CONAMA) - Ministério do Meio Ambiente. *Diário Oficial da União*, Brasília, DF, 2009.
- CHEN, Q.Y.; TYRER, M.; HILLS, C.D.; YANG, X.M.; CAREY, P. Immobilization of heavy metal in cement-based solidification/stabilization: a review. *Waste Manag.*, v. 29, n. 1, p. 390 - 403, 2009. <https://doi.org/10.1016/j.wasman.2008.01.019>
- DELMONTE, B.A. *Caracterização geoambiental da Cia Mercantil e Industrial Ingá*. 2010. 138 f. Dissertação (Mestrado em Engenharia Civil) - Pontifícia Universidade Católica do Rio de Janeiro, Rio de Janeiro, 2010.
- DU, Y.J.; HORPIBULSUK, S.; WEI, M.L.; SUKSIRIPATTANAPONG, C.; LIU, M.D. Modeling compression behavior of cement-treated zinc-contaminated clayey soils. *Soils and Found.*, v. 54, n. 5, p. 1018 - 1026, 2014a. <https://doi.org/10.1016/j.sandf.2014.09.007>
- DU, Y.J.; JIANG, N.J.; LIU, S.Y.; JIN, F.; SINGH, D.N.; PUPPALA, A.J. Engineering properties and microstructural characteristics of cement-stabilized zinc-contaminated kaolin. *Canadian Geotech. J.*, v. 51, n. 3, p. 289 - 302, 2014b. <https://doi.org/10.1139/cgj-2013-0177>
- DU, Y.J.; WEI, M.L.; JIN, F.; LIU, Z.B. Stress-strain relation and strength characteristics of cement treated zinc-contaminated clay. *Eng. Geol.*, v. 167, p. 20 - 26, 2013. <https://doi.org/10.1016/j.enggeo.2013.10.005>
- DUCE, J.A.; TSATSANIS, A.; CATER, M.A. *et al.* Iron-export ferroxidase activity of β -amyloid precursor protein is inhibited by zinc in Alzheimer's disease. *Cell*, v. 142, n. 6, p. 857 - 867, 2010. <https://doi.org/10.1016/j.cell.2010.08.014>
- ENVIRONMENTAL PROTECTION AGENCY. *A citizen's guide to solidification and stabilization*. EPA: Washington, DC, 2017. Available at: <https://19january2017snapshot.epa.gov/remedytech/citizens-guide-solidification-and-stabilization_html>. Accessed on: 31 mar. 2022.
- GLASSER, F.P. Fundamental aspects of cement solidification and stabilization. *J. Hazard. Mater.*, v. 52, n. 2 - 3, p. 151 - 170, 1997. [https://doi.org/10.1016/S0304-3894\(96\)01805-5](https://doi.org/10.1016/S0304-3894(96)01805-5)
- HALE, B.; EVANS, L.; LAMBERT, R. Effects of cement or lime on Cd, Co, Cu, Ni, Pb, Sb and Zn mobility in field-contaminated and aged soils. *J. Hazard. Mater.*, v. 199 - 200, p. 119 - 127, 2012. <https://doi.org/10.1016/j.jhazmat.2011.10.065>
- HORNING, M.S.; BLAKEMORE, L.J.; TROMBLEY, P.Q. Endogenous mechanisms of neuroprotection: role of zinc, copper, and carnosine. *Brain Res.*, v. 852, n. 1, p. 56 - 61, 2000. [https://doi.org/10.1016/S0006-8993\(99\)02215-5](https://doi.org/10.1016/S0006-8993(99)02215-5)
- JIANG, N.J.; DU, Y.J.; LIU, S.Y.; ZHU, J.J. Experimental investigation of the compressibility behavior of cement-solidified/stabilized zinc-contaminated kaolin clay. *Geotech. Letters*, v. 4, n. 1, p. 27 - 32, 2014. <https://doi.org/10.1680/geolett.13.00079>
- KEMPA, T.; MARSCHALKO, M.; YILMAZ, I.; LACKOVÁ, E. *et al.* In-situ remediation of the contaminated soils in Ostrava city (Czech Republic) by steam curing/vapor. *Eng. Geol.*, v. 154, p. 42 - 55, 2013. <https://doi.org/10.1016/j.enggeo.2012.12.008>
- KLIMEK, B. Effect of long-term zinc pollution on soil microbial community resistance to repeated contamination. *Bull. Environ. Contam. Toxicol.*, v. 88, n. 4, p. 617 - 622, 2012. <https://doi.org/10.1007/s00128-012-0523-0>
- KNOP, A.; VANGULCK, J.; HEINECK, K.S.; CONSOLI, N.C. Compacted artificially cemented soil-acid leachate contaminant interactions: breakthrough curves and transport parameters. *J. Hazard. Mater.*, v. 155, n. 1 - 2, p. 269 - 276, 2008. <https://doi.org/10.1016/j.jhazmat.2007.11.056>
- LI, J.; HASHIMOTO, Y.; RIYA, S.; TERADA, A.; HOU, H.; SHIBAGAKI, Y.; HOSOMI, M. Removal and immobilization of heavy metals in contaminated soils by

- chlorination and thermal treatment on an industrial-scale. *Chem. Eng. J.*, v. 359, p. 385 - 392, 2019. <https://doi.org/10.1016/j.cej.2018.11.158>
- LIU, J.; ZHA, F.; XU, L.; YANG, C.; CHU, C.; TAN, X. Effect of chloride attack on strength and leaching properties of solidified/stabilized heavy metal contaminated soils. *Eng. Geol.*, v. 246, p. 28 - 35, 2018. <https://doi.org/10.1016/j.enggeo.2018.09.017>
- LOUZADA, N.D.S.L.; MALKO, J.A.C.; CASAGRANDE, M.D.T. Behavior of clayey soil reinforced with polyethylene terephthalate. *J. Mater. Civ. Eng.*, v. 31, n. 10, p. 04019218, 2019. [https://doi.org/10.1061/\(ASCE\)MT.1943-5533.0002863](https://doi.org/10.1061/(ASCE)MT.1943-5533.0002863)
- MCKINLEY, J.D.; THOMAS, H.R.; WILLIAMS, K.P.; REID, J.M. Chemical analysis of contaminated soil strengthened by the addition of lime. *Eng. Geol.*, v. 60, n. 1 - 4, p. 181 - 192, 2001. [https://doi.org/10.1016/S0013-7952\(00\)00100-9](https://doi.org/10.1016/S0013-7952(00)00100-9)
- NEWSOME, L.; MORRIS, K.; LLOYD, J.R. The biogeochemistry and bioremediation of uranium and other priority radionuclides. *Chem. Geol.*, v. 363, p. 164 - 184, 2014. <https://doi.org/10.1016/j.chemgeo.2013.10.034>
- NIU, M.; LI, G.; WANG, Y.; LI, Q.; HAN, L.; SONG, Z. Comparative study of immobilization and mechanical properties of sulfoaluminate cement and ordinary Portland cement with different heavy metals. *Constr. Build. Mater.*, v. 193, p. 332 - 343, 2018. <https://doi.org/10.1016/j.conbuildmat.2018.10.206>
- OLMO, I.F.; CHACON, E.; IRABIEN, A. Influence of lead, zinc, iron (III) and chromium (III) oxides on the setting time and strength development of Portland cement. *Cem. Concr. Res.*, v. 31, n. 8, p. 1213 - 1219, 2001. [https://doi.org/10.1016/S0008-8846\(01\)00545-2](https://doi.org/10.1016/S0008-8846(01)00545-2)
- PEDERSEN, K.B.; JENSEN, P.E.; OTTOSEN, L.M.; BARLINDHAUG, J. The relative influence of electrokinetic remediation design on the removal of As, Cu, Pb and Sb from shooting range soils. *Eng. Geol.*, v. 238, p. 52 - 61, 2018. <https://doi.org/10.1016/j.enggeo.2018.03.005>
- PEREZ, I.A. *Evaluation of the encapsulation potential of a contaminated soil with zinc chloride through the lime and cement addition*. Pontifical Catholic University of Rio de Janeiro, Brazil, 2017. Accessed on: 31 mar. 2020. <https://doi.org/10.17771/PUCRio.acad.31398>
- RAMIREZ, G.G.D.; CASAGRANDE, M.D.T.; FOLLE, D.; PEREIRA, A.; PAULON, V. A. Behavior of granular rubber waste tire reinforced soil for application in geosynthetic reinforced soil wall. *Rev. IBRACON Estrut. e Mater.*, v. 8, p. 567 - 576, 2015. <https://doi.org/10.1590/S1983-41952015000400009>
- SCRIVENER, K.; OUZIA, A.; JUILLAND, P.; MOHAMED A.K. Advances in understanding cement hydration mechanisms. *Cem. Concr. Res.*, v. 124, p. 105823, 2019. <https://doi.org/10.1016/j.cemconres.2019.105823>
- WEI, M.; DU, Y.; ZHANG, F. Fundamental properties of strength and deformation of cement solidified/stabilized zinc contaminated soils. *Rock and Soil Mech.*, v. 32, n. 2, p. 306 - 312, 2011.
- WEI, M.L.; DU, Y.J.; JIANG, N.J. Compression behavior of zinc contaminated clayey soils solidified with cement. In: *GeoCongress, 2012. American Society of Civil Engineers*. Reston, VA, p. 4042 - 4049. <https://doi.org/10.1061/9780784412121.415>
- YIN, C.Y.; MAHMUD, H.B.; SHAABAN, M.G. Stabilization/solidification of lead-contaminated soil using cement and rice husk ash. *J. Hazard. Mater.*, v. 137, n. 3, p. 1758 - 1764, 2006. <https://doi.org/10.1016/j.jhazmat.2006.05.013>
- YOUSUF, M.; MOLLAH, A.; VEMPATI, R.K.; LIN, T.C.; COCKE, D.L. The interfacial chemistry of solidification/stabilization of metals in cement and pozzolanic material systems. *Waste Manag.*, v. 15, n. 2, p. 137 - 148, 1995. [https://doi.org/10.1016/0956-053X\(95\)00013-P](https://doi.org/10.1016/0956-053X(95)00013-P)